36th International Electric Vehicle Symposium and Exhibition (EVS36)
Sacramento, California, USA, June 11-14, 2023

Multi-Channel Multi-Frequency Wireless Power Transfer System for Automated Guided Vehicles

Songtao Li[1], K. T. Chau[1], Wei Liu[1], Chunhua Liu[2] and Yongbin He[3]

[1] *Department of Electrical and Electronic Engineering, The University of Hong Kong, Hong Kong, China (Email: ktchau@eee.hku.hk)*

[2] *School of Energy and Environment, City University of Hong Kong, Hong Kong, China*

[3] *BYD Co. Ltd., Shenzhen, China*

Executive Summary

This paper proposes a multi-channel multi-frequency wireless power transfer (MCMF-WPT) system for automated guided vehicles (AGVs). In particular, a double-channel double-frequency wireless separately excited DC motor is proposed, which can enable AGVs working continuously for delivery in warehouses without any timeout for battery charging. Generally, wireless motors using multi-channel transmissions require multiple wireless power transmitters or receivers, which will occupy larger space and reduce cost-effectiveness while leading to less compactness. By using one magnetic coupler only, the proposed MCMF-WPT system can energize multi-loads flexibly and compactly. Moreover, the proposed system adopts the damping filters to successfully suppress the cross-interference between neighboring channels at the receiver side, while a high order compensation is configured to achieve full resonances at the transmitter side. In such a way, the WPT outputs of different channels can be controlled separately for fitting different operating conditions. Finally, both theoretical analysis and computer simulation are provided to verify the feasibility of the proposed MCMF-WPT system for a double-channel double-frequency wireless separately excited DC motor.

Keywords: Multi-frequency multi-channel, separately excited dc motor, single magnetic coupler, speed control, wireless power transfer

1 Introduction

Wireless power transfer (WPT) is identified as one of the most epoch-making technologies in recent years. Based on the mechanism of magnetic resonance coupling [1], the WPT delivers power without wires, thus having numerous advantages of great flexibility [2-4], high security [5, 6], and maintenance-free [7, 8] in various applications, such as portable electric devices [9, 10], medical implants [11, 12], and electric vehicles (EVs) [13-15]. In recent years, automated guided vehicles (AGVs) are widely applied in industries for delivering [16, 17]. However, due to the limited energy capacity of batteries, regular charging is needed by taking a long time, thus interrupting the operation of AGVs [18].

After years of research, WPT schemes were actively explored to power and control electric motors directly [19-22]. Therefore, the batteries of AGVs are no longer needed, which allows AGVs to work continuously. The concept of wireless motor was first proposed to avoid cable disconnection in harsh environments [23]. However, the dual-controller and dual-inverter structure brings high complexity and maintenance needs. Similar topologies were also presented in the literature [24-26]. To eliminate the controller on the motor side, the self-driving inverter was introduced into the receiver circuit, which realized switching control and power transmission simultaneously [27, 28]. Compared with passive components, active switches are still vulnerable.

To eliminate the active power switches at the receiver side, the multi-channel WPT system is used for wireless motors. Firstly, a wireless switched reluctance (SR) motor using decoupled coils was revealed [20]. Wherein, each phase of the wireless SR motor was powered by an independent WPT channel, while the decoupled coils were deployed to prevent interference. However, the decoupling coupler is sensitive to misalignment, which limits its application in moving objects like AGVs. By utilizing multiple resonant frequencies, the WPT can provide multiple power channels with a single transmitter [29-31], which enables energizing the multi-phase loads selectively or simultaneously while offering independently controlled capability. Secondly, a wireless separately excited DC motor using time-division multiplexing was studied [32], and its armature and field windings were powered alternatively in a short period to realize the individual control, but its output power and control precision were sacrificed slightly due to the multiplexing.

In this paper, the main purpose is to present a multi-channel multi-frequency (MCMF) WPT system for Automated Guided Vehicles. Particularly, a double-frequency double-channel wireless separately excited DC motor is proposed based on the MCMF-WPT scheme. The armature and field windings can be energized and controlled independently by using a single transmitter to fully utilize the speed range.

2 Multi-channel Multi-frequency WPT system

The proposed MCMF-WPT scheme provides the ability to energize multiple loads with different input levels, by utilizing a single transmitter, a more compact size can be achieved, which shows great potential in the direct drive of robotics and EVs. The proposed MCMF-WPT system is depicted in Fig. 1. The inverters generate powers composing different frequency components to energize the multi-frequency transmitter network. The compensation circuits at both the transmitter side and receiver side are tuned at different resonant frequencies for higher efficiency and better selectability. To reduce the eliminate the cross-interference caused by unrelated channels, damping filters are adopted in each channel. Therefore, by

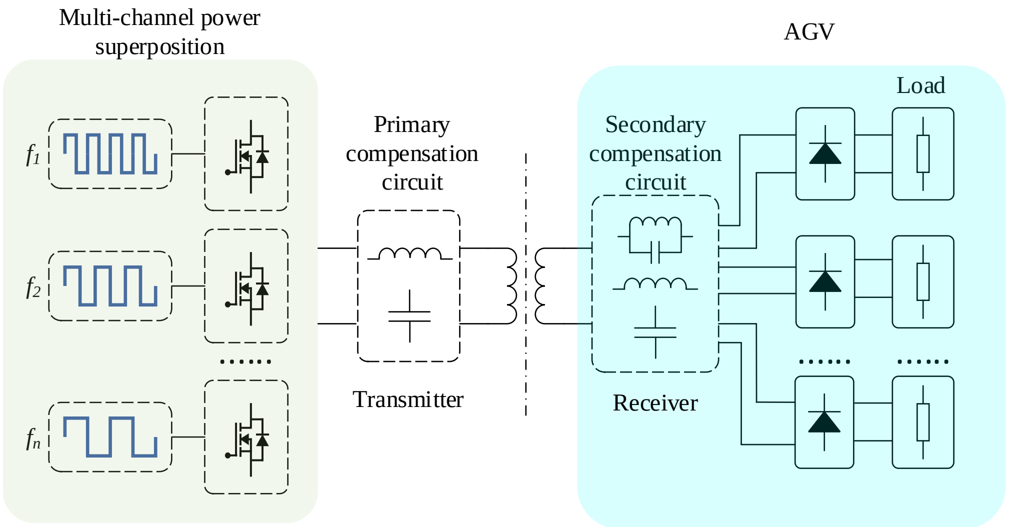

Figure1: Proposed MCMF-WPT system using a single magnetic coupler.

regulating the fundamental component of each channel, the output of each load can be controlled independently.

3 Wireless separately excited DC motor using MCMF-WPT

Based on the MCMF-WPT scheme, a double-channel double-frequency separately excited DC motor is investigated, as shown in Fig. 2. A full bridge inverter is utilized to generate power composing two fundamental components with different frequencies f_1 and f_2, respectively. The power is transmitted through a shared magnetic coupler, then separate into two channels in the receiver side. Channel 1 is connected to the armature winding, and channel 2 is connected to the field winding. Meanwhile, Since only one receiver is involved, each channel is connected with one damping filter so as to reduce the cross-interference between neighboring channels. To achieve resonant conditions on both channels, dual-frequency compensation scheme is adopted as variable capacitors in the transmitter circuit [33]. Thus, the voltage and current of each winding can be controlled individually and precisely, providing a wide speed range.

3.1 Principle of multi-channel power superposition

The operating frequency of switches S_1 and S_2 is f_1, while that of S_3 and S_4 is f_2 [34]. Fig. 3 shows the theoretical waveform of the inverter output voltage. The inverter output voltage is

$$u_{AB} = u_A - u_B \tag{1}$$

where u_A and u_B can be calculated by using Fourier expansion, n represents the order of harmonics, δ_{d1} and

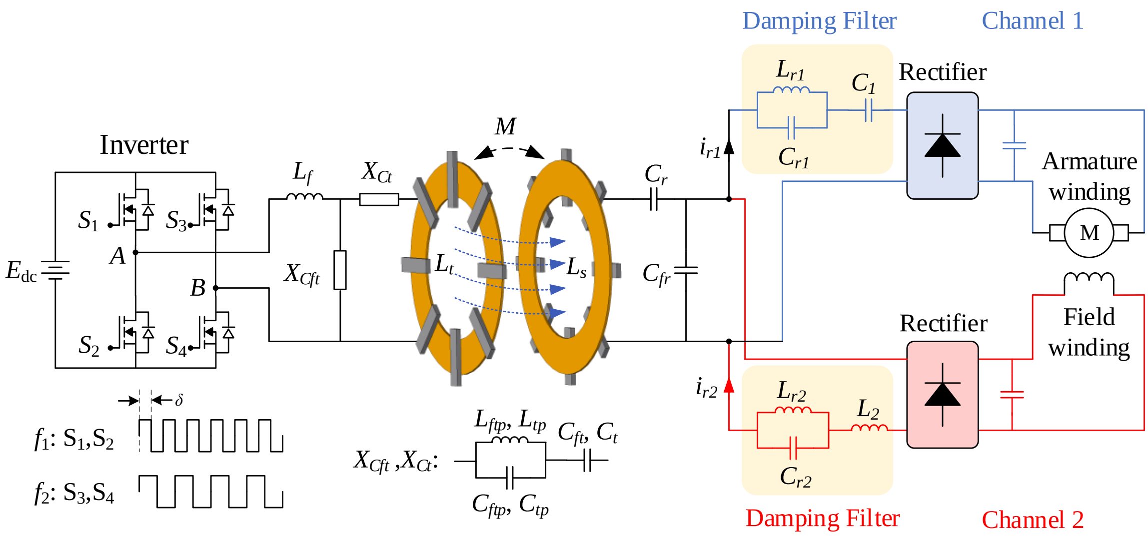

Figure2: Proposed MCMF-WPT system using a single magnetic coupler.

δ_{d2} denote the duty ratio of PWM in each channel.

$$\begin{aligned} u_A &= \frac{D_1 E_{dc}}{T_1} + \sum_{n=1}^{\infty} \frac{2E_{dc}}{n\pi} \sin(n\pi\delta_{d1}) \cos(n\omega_1 t) \\ u_B &= \frac{D_2 E_{dc}}{T_2} + \sum_{n=1}^{\infty} \frac{2E_{dc}}{n\pi} \sin(n\pi\delta_{d2}) \cos(n\omega_2 t) \end{aligned} \tag{2}$$

For the proposed WPT system, only the fundamental AC component is considered, which can be expressed as

$$u_{AB1} = \frac{2E_{dc}}{\pi} \sin(\pi\delta_{d1}) \cos(\omega_1 t) - \frac{2E_{dc}}{\pi} \sin(\pi\delta_{d2}) \cos(\omega_2 t) \tag{3}$$

Therefore, the output is the superposition of two power channels in two frequencies of f_1 and f_2, and the amplitude can be controlled using pulse-width modulation (PWM) to separately control the output current by changing the duty ratio δ_{d1},δ_{d2}. Correspondingly, the output current can be managed individually. When the duty ratio is set at 0.5, the fundamental component of inverter output voltage reaches its peak value, and the output will be zero when equal to 0 or 1, theoretically.

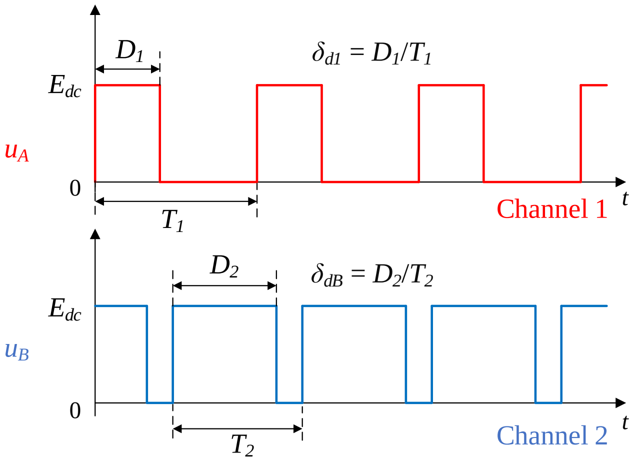

Figure3: Theoretical waveform of inverter output voltage

3.2 Magnetic Coupler Design

The magnetic coupler in the WPT system should provide maximum transfer distance and high efficiency. For the WPT system using a single coil, both rectangular coil structure and circular coil structure were adopted in the previous studies [35, 36]. Compared with the circular coil structure, the rectangle coil structure suffers from lower mutual inductance using the same weight and length of wires and the same transfer distance [37]. Therefore, a circular coil structure is used for the magnetic coupler in the proposed system. To further strengthen the magnetic coupling under the same distance, eight ferrite bars with a size of 60 × 15 × 5 mm are laid at the top of the receiver coil and bottom of the transmitter coil. The material of the ferrite bars is PC95. Fig. 4 shows the detailed geometric dimension of the magnetic coupler.

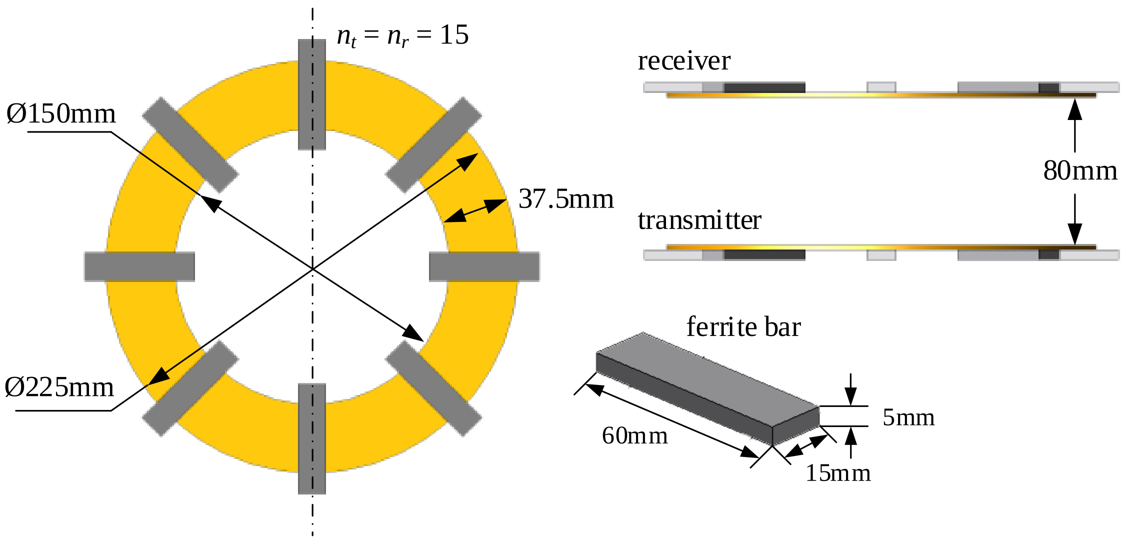

Figure4: Geometric dimension of transmitter and receiver coils

3.3 System Characteristics and Analysis

The equivalent circuit of the proposed wireless separately excited DC motor is shown in Fig. 5, where the field winding and armature winding are simplified to resistors. u_s is the power source, L_f denote the filter inductance, X_{Cft} and X_{Ct} represent the variable filter capacitance and matched capacitance of the transmitter under two operating frequencies; C_r, C_{fr} represent the matched capacitance and filter capacitance of the receiver; L_t, L_s are the transmitter and receiver coil inductances; L_{rk}, C_{rk} (k = 1, 2) compose two band-stop filters which the stopband centered at f_1 and f_2. The impedance of the band-stop filters can be calculated as

$$Z_{p1} = \frac{j\omega L_{r1}}{1-\omega^2 L_{r1} C_{r1}}$$
$$Z_{p2} = \frac{j\omega L_{r2}}{1-\omega^2 L_{r2} C_{r2}} \tag{4}$$

Z_{rc1}, Z_{rc2} are the compensation components for resonance, the type is defined by the impedance of other components at the resonant frequency.

The compensation circuit adopts a T-type structure [28] on both the transmitter and receiver sides. Since the two power channels share the same route before the damping filters, the values of components are tuned to provide desired outputs. The receiver circuit is tuned to form a symmetrical T-type structure for channel 2, to provide a constant voltage / current output, which is defined by the transmitter circuit. The relation is shown in equation (5). When working at frequency f_2, Z_{p2} is capacitive, Z_{rc2} should be inductive, which can be represented by an inductor L_2.

$$j\omega_2 L_s + \frac{1}{j\omega_2 C_r} = \frac{j\omega_2 L_{r2}}{1-\omega_2^2 L_{r2} C_{r2}} + Z_{rc2} = -\frac{1}{j\omega_2 C_{fr}}, \qquad Z_{rc2} = j\omega_2 L_2 \tag{5}$$

The input impedance of the receiver circuit is resistive at frequency f_2

$$Z_{z2} = \frac{1}{\omega_2^2 C_{fr}^2 R_{Le2}} \tag{6}$$

The equivalent impedance of channel 2 at the transmitter circuit is

$$Z_{eq2} = \omega_2^4 C_{fr}^2 R_{Le2} M^2 \tag{7}$$

For channel 1, when working at frequency f_1, the parameters are tuned as

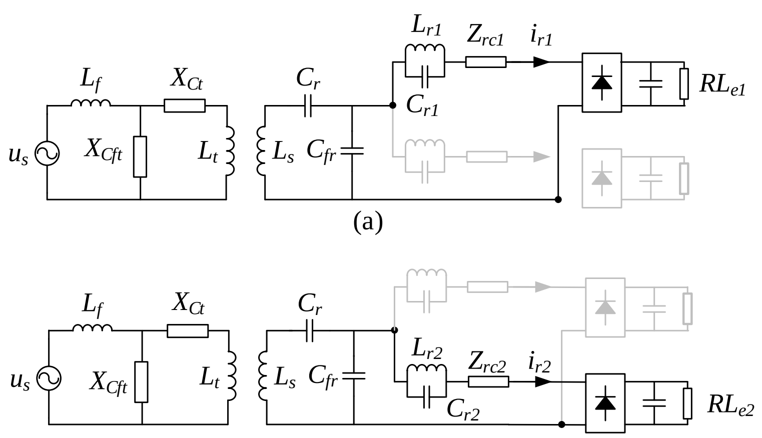

Figure5: Equivalent circuit of the proposed MCMF-WPT system in different channels. (a) Channel 1. (b) Channel 2.

$$\frac{j\omega_1 L_{r1}}{1-\omega_1^2 L_{r2} C_{r1}} + Z_{rc1} = j\omega_2 L_1 + \frac{1}{j\omega_1 C_r} = 0, \qquad Z_{rc1} = \frac{1}{j\omega_1 C_1} \tag{8}$$

The input impedance is not resistive due to the unsymmetrical T-type structure, shown as

$$Z_{z1} = \frac{R_{Le1}}{1 + j\omega_1 C_{fr} R_{Le2}} \tag{9}$$

Therefore, the equivalent impedance of channel 1 at the transmitter circuit is

$$Z_{eq1} = \frac{\omega_1^2 M^2}{R_{Le}} + j\omega_1^3 C_{fr} M^2 \tag{10}$$

which is the sum of a resistive component and an inductive component. However, the inductive component is unrelated to the load, which makes the resonant status unchanged with a variable load, such as an electric motor. The transmitter circuit provides two resonant frequencies f_1 and f_2 in a T-type LCC compensation structure. The equivalent capacitances of X_{Cft}, X_{Ct} and the parameters of LC components in the equivalent capacitors can be calculated using the relations

$$\begin{cases} j\omega_1 L_f = -\dfrac{1}{j\omega_1 X_{Cft}^{(\omega_1)}} = j\omega_1\left(L_t + \omega_1^2 M^2 C_{fr}\right) - \dfrac{1}{j\omega_1 X_{Ct}^{(\omega_1)}} \\ j\omega_2 L_f = -\dfrac{1}{j\omega_2 X_{Cft}^{(\omega_2)}} = j\omega_2 L_t - \dfrac{1}{j\omega_2 X_{Ct}^{(\omega_2)}} \end{cases} \tag{11}$$

$$\begin{cases} \dfrac{j\omega_k L_{ftp}}{1-\omega_k^2 L_{ftp} C_{ftp}} + \dfrac{1}{j\omega_k C_{ft}} = \dfrac{1}{j\omega_k X_{Cftk}^{(\omega_k)}} \\ \dfrac{j\omega_k L_{tp}}{1-\omega_k^2 L_{tp} C_{tp}} + \dfrac{1}{j\omega_k C_t} = \dfrac{1}{j\omega_k X_{Ctk}^{(\omega_k)}} \end{cases} \tag{12}$$

As shown in [30], the current in the transmitter coil is

$$\begin{aligned} I_{t1} &= \frac{u_s}{j\omega_1 L_f} \\ I_{t2} &= \frac{u_s}{j\omega_2 L_f} \end{aligned} \tag{12}$$

which keeps a constant value under a constant voltage source. Therefore, the output voltage of channel 1 and output current of channel 2 are constant against variation of load [38].

4 Verification and Results

To verify the feasibility of the proposed MCMF-WPT system, a finite element analysis (FEA) model was built for evaluation, where the geometric dimensions of the magnetic coupler are presented in detail in Fig. 4. A circuit model was built using the parameters shown in Table I. Wherein, the operating frequencies are selected as 120 kHz and 180 kHz. The magnetic field distribution with a constant current input of 10 A and a 25 Ω resistive load on both channels is depicted in Fig. 6, with the same circuit parameters in Table 1. Fig. 7 shows the input impedance characteristics with different load values. The results show that the input impedance angle remains zero against the variation of load.

To better identify and evaluate the regulation performance of outputs, the wireless motor was represented by using resistive loads of 25 Ω, and the DC voltage source is set at 80 V. Fig. 8 (a) and (b) shows the load voltage when decreasing the output in only one channel, while keeping maximum output in another channel. The results show that the output can be controlled flexibly by changing the duty ratio of the inverter output, while that of the non-targeted channel keeps nearly unaffected. Fig. 8 (c) and (d) depict the AC current variation of the controlled channel, which well verifies that the cross-coupling interference can be effectively suppressed and the controllability of the proposed system.

To assess the practical performance of the proposed motor, a circuit model is built according to Fig. 2. The armature winding is powered by the 120-kHz channel, while that of the field winding is connected to the 180-kHz channel. The rated input voltage of the wireless motor is 240 V, and the rated speed is 1750 rpm. Fig. 9 shows the motor speeds with respect to different duty ratios of armature and field winding under a constant load torque of 1 N.m. When the duty ratio of the 120-kHz channel is 0.5 and 0.1 for the other channel, the motor speed can reach its rated speed with an output torque of 1 N.m. Lowering the armature voltage can reduce the motor speed, while a higher speed can be obtained by reducing the field winding current through the flux-weakening control. Hence, the proposed wireless motor system has a wide speed range.

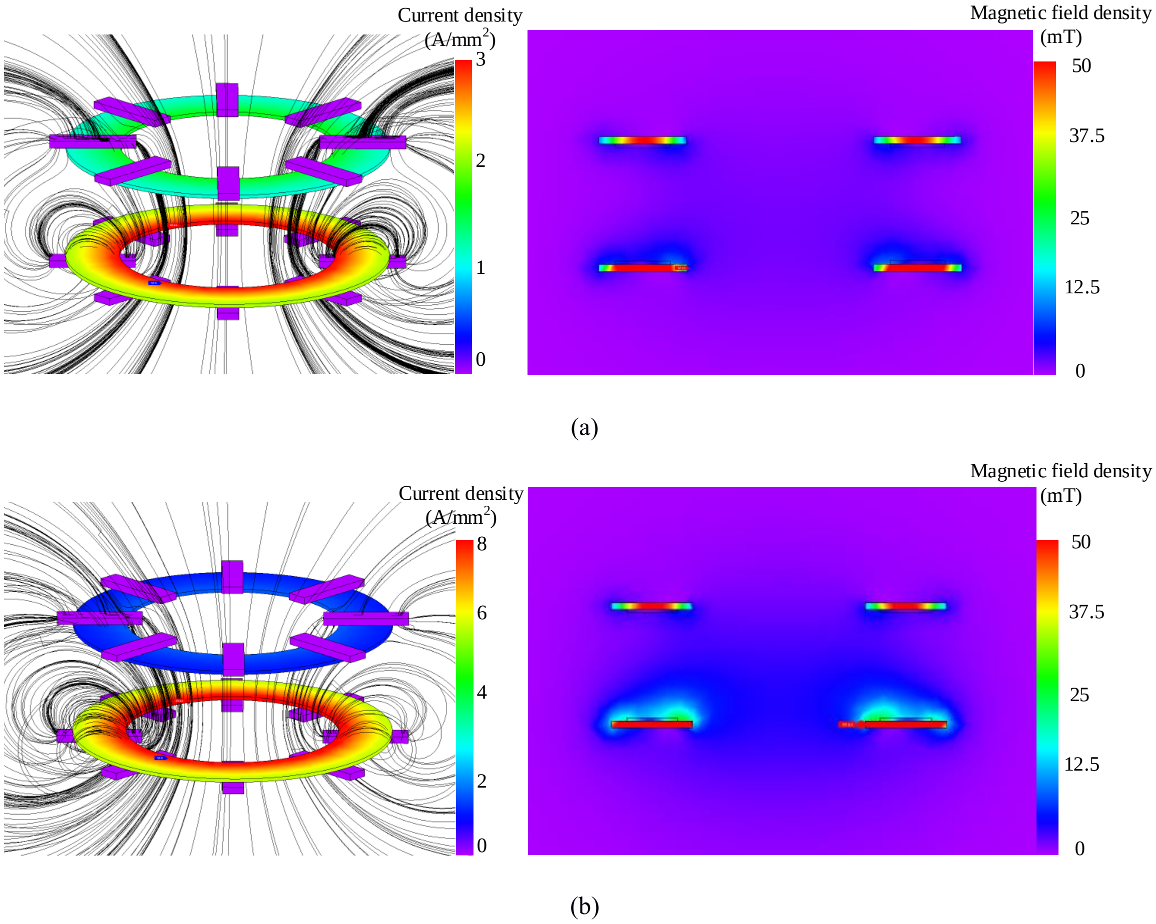

Figure6: Magnetic flux distribution of transmitter and receiver coils under working frequencies of 120 kHz and 180 kHz. (a) 120 kHz (b) 180 kHz

5 Conclusion

This paper proposes a multi-channel multi-frequency WPT system for AGVs, particularly, a double-channel double-frequency wireless separately excited DC motor is proposed. The proposed motor can be powered and driven by using WPT directly, which can enable AGVs working continuously in warehouses without the need for any battery modules. Using only one magnetic coupler, the size of the system can be reduced. The proposed system utilized high-order compensation to achieve resonant conditions under different frequencies, and damping filters to eliminate interference between the two channels. Using the proposed scheme, the two power channels can achieve independent control, therefore, the speed of the proposed motor has a wide speed range, and the speed can be regulated conveniently by changing the duty ratio. The feasibility of the proposed motor is verified by both theoretical analysis and computer simulation.

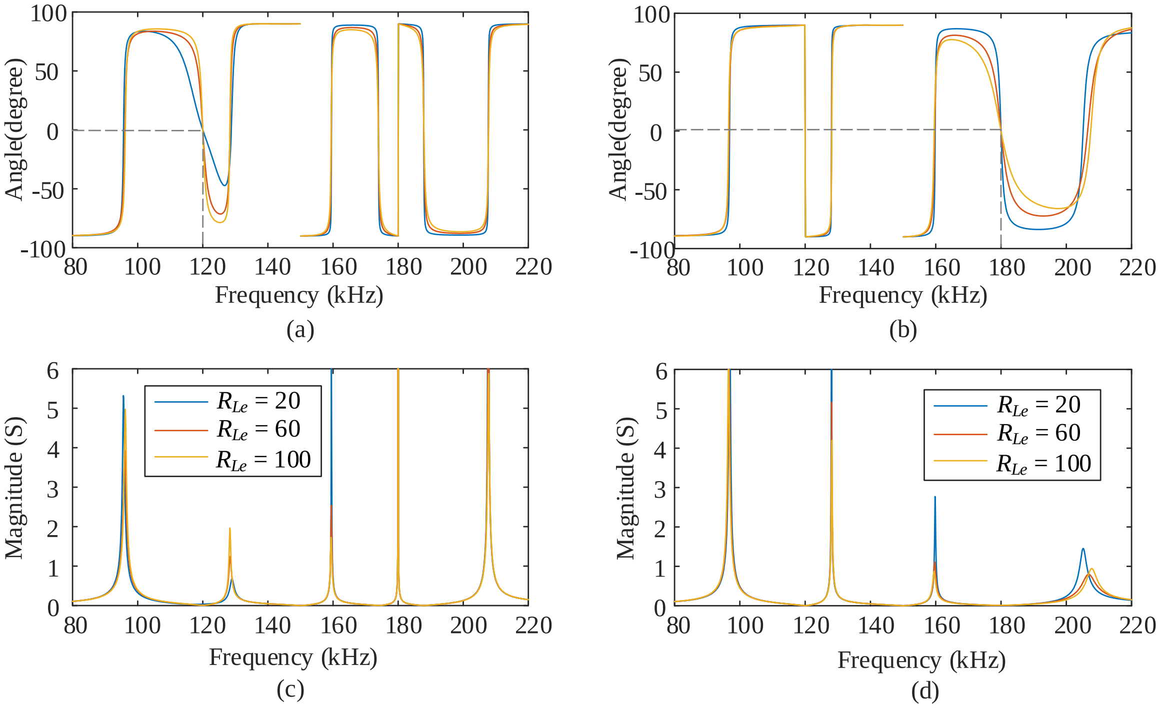

Figure7: Input impedance characteristics under operating frequencies f_1 and f_2. (a) Impedance angle working under f_1. (2) Impedance angle working under f_2. (3) Transconductance under f_1. (4) Transconductance under f_2.

Table 1: Simulation parameters

Items	Value
Transmitter coil inductance (L_t)	81.67 µH
Operating frequencies (f_1, f_2)	120 kHz, 180 kHz
Transmitter filter inductance (L_f)	20 µH
Variable capacitor X_{Cft} parameters (L_{ftp}, C_{ftp}, C_{ft})	3.17 µH, 355.36 nF, 61.08 nF
Variable capacitor X_{Ct} parameters (L_{tp}, C_{tp}, C_t)	9.40 µH, 119.70 nF, 19.40 nF
Receiver coil inductance (L_r)	81.67 µH
Receiver matched capacitance (C_r)	21.54 nF
Receiver filter capacitance (L_{fr})	17.23 nF
Channel 1 damping filter parameters (L_{r1}, C_{r1}, C_1)	30 µH, 26.06 nF, 32.57 nF
Channel 2 damping filter parameters (L_{r2}, C_{r2}, L_2)	30 µH, 58.63 nF, 69.37 µH

Acknowledgments

This work was fully supported by a grant from the Hong Kong Research Grants Council, Hong Kong Special Administrative Region, China, under Project No. T23-701/20-R.

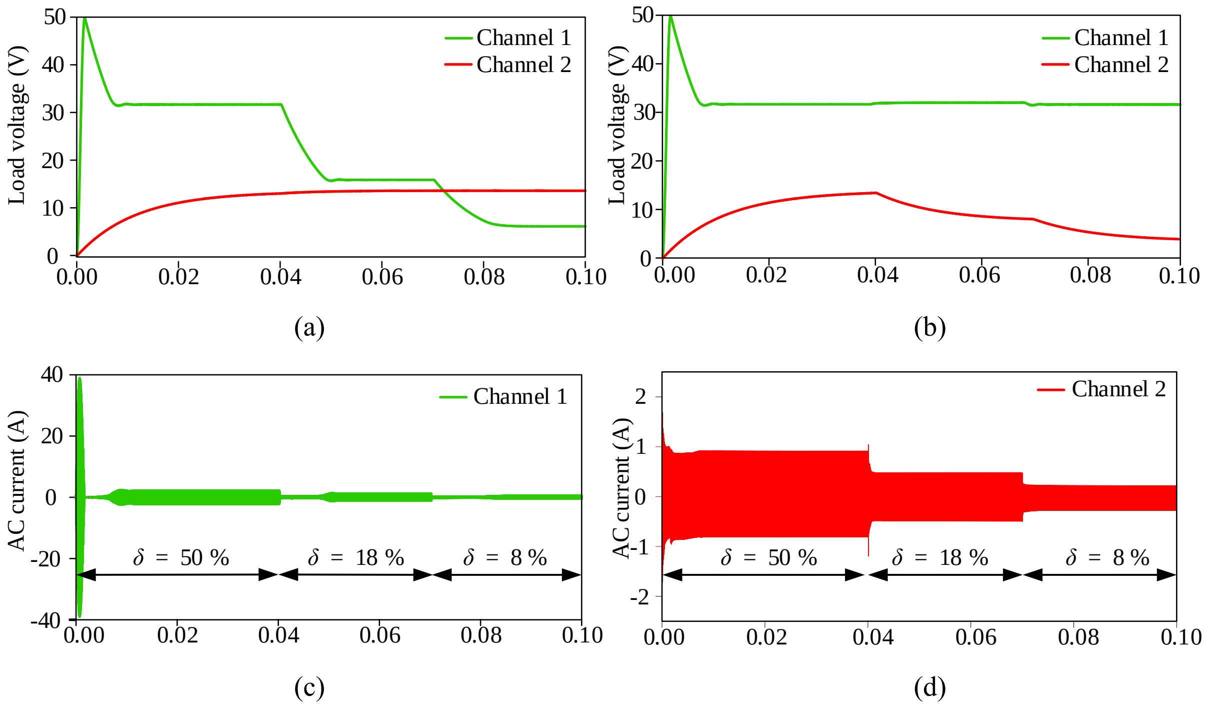

Figure8: Decoupled regulation of proposed MCMF-WPT system using PWM. (a) Load voltage of both channels when decreasing duty ratio in channel 1. (b) Load voltage of both channels when decreasing duty ratio in channel 2. (c) Load current of channel 1 when decreasing duty ratio. (d) Load current of channel 2 when decreasing duty

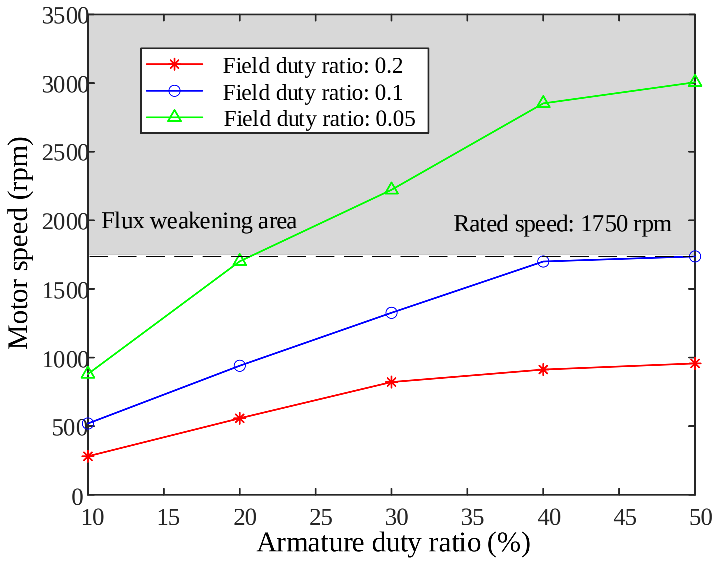

Figure9: Speed control performance of proposed double-channel double-frequency wireless separately excited DC motor.

References

[1] C. Qiu, K. T. Chau, T. W. Ching, and C. Liu, *Overview of wireless charging technologies for electric vehicles*, Journal of Asian Electric Vehicles, ISSN 1883-6038, 12(2014), 1679-1685.

[2] X. Tian, K. T. Chau, W. Liu and C. H. T. Lee, *Selective wireless power transfer using magnetic field editing*, IEEE Transactions on Power Electronics, ISSN 1941-0107, 36(2021), 2710-2719.

[3] J. -Q. Zhu, Y. -L. Ban, Y. Zhang, Z. Yan, R. -M. Xu and C. C. Mi, *Three-Coil wireless charging system for metal-cover smartphone applications*, IEEE Transactions on Power Electronics, ISSN 1941-0107, 35(2020), 4847-4858.

[4] C. Liu, C. Jiang, J. Song and K. T. Chau, *An effective sandwiched wireless power transfer system for charging implantable cardiac pacemaker*, IEEE Transactions on Industrial Electronics, ISSN 1557-9948, 66(2019), 4108-4117.

[5] W. Liu, K. T. Chau, C. H. T. Lee, C. Jiang and W. Han, *A switched-capacitorless energy-encrypted transmitter for roadway-charging electric vehicles*, IEEE Transactions on Magnetics, ISSN 1941-0069, 54(2018), 1-6.

[6] Z. Zhang, K. T. Chau, C. Qiu and C. Liu, *Energy encryption for wireless power transfer*, IEEE Transactions on Power Electronics, ISSN 1941-0107, 30(2015), 5237-5246.

[7] C. Jiang, K. T. Chau, C. H. T. Lee, W. Han, W. Liu and W. H. Lam, *A wireless servo motor drive with bidirectional motion capability*, IEEE Transactions on Power Electronics, ISSN 1941-0107, 34(2019), 12001-12010.

[8] C. Jiang, K. T. Chau, C. Liu and W. Han, *Design and analysis of wireless switched reluctance motor drives*, IEEE Transactions on Industrial Electronics, ISSN 1557-9948, 66(2019), 245-254.

[9] W. Han, K. T. Chau, and Z. Zhang, *Flexible induction heating using magnetic resonant coupling*, IEEE Transactions on Industrial Electronics, ISSN 1557-9948, 64(2017), 1982-1992.

[10] H. Hoang, S. Lee, Y. Kim, Y. Choi and F. Bien, *An adaptive technique to improve wireless power transfer for consumer electronics*, IEEE Transactions on Consumer Electronics, ISSN 1558-4127, 58(2012), 327-332.

[11] Y. Zhou, C. Liu, and Y. Huang, *Wireless power transfer for implanted medical application: a review*, Energies, ISSN 1996-1073, 13(2020), 2837-2867.

[12] Q. Wang, W. Che, M. Mongiardo and G. Monti, *Wireless power transfer system with high misalignment tolerance for bio-medical implants*, IEEE Transactions on Circuits and Systems II: Express Briefs, ISSN 1558-3791, 67(2020), 3023-3027.

[13] S. Niu, H. Xu, Z. Sun, Z.Y. Shao, L. Jian, *The state-of-the-arts of wireless electric vehicle charging via magnetic resonance: principles, standards and core technologies*, Renewable and Sustainable Energy Reviews, ISSN 1364-0321, 114(2019), 109302.

[14] W. Liu, T. Placke, and K. T. Chau, *Overview of batteries and battery management for electric vehicles*, Energy Reports, ISSN 2352-4847, 8(2022), 4058-4084.

[15] C. -C. Huang, C. -L. Lin and Y. -K. Wu, *Simultaneous wireless power/data transfer for electric vehicle charging*, IEEE Transactions on Industrial Electronics, ISSN 1557-9948, 64(2017), 682-690.

[16] Y. Lian, Q. Yang, W. Xie and L. Zhang, *Cyber-physical system-based heuristic planning and scheduling method for multiple automatic guided vehicles in logistics systems*, IEEE Transactions on Industrial Informatics, ISSN 1941-0050, 17(2021), 7882-7893.

[17] Q. Zou, Q. Sun, L. Chen, B. Nie and Q. Li, *A comparative analysis of lidar slam-based indoor navigation for autonomous vehicles*, IEEE Transactions on Intelligent Transportation Systems, ISSN 1558-0016 23(2022), 6907-6921.

[18] C. Jiang, K. T. Chau, C. Liu, C. H. T. Lee, W. Han and W. Liu, *Move-and-charge system for automatic guided vehicles*, IEEE Transactions on Magnetics, ISSN 1941-0069, 54(2018), 1-5.

[19] W. Liu, K. T. Chau, C. H. T. Lee, L. Cao and C. Jiang, *Frequency-modulated wireless direct-drive motor control*, IEEE Transactions on Magnetics, ISSN 1941-0069, 57(2021), 1-7.

[20] H. Wang, K. T. Chau, C. H. T. Lee and X. Tian, *Design and analysis of wireless resolver for wireless switched reluctance motors*, IEEE Transactions on Industrial Electronics, ISSN 1557-9948, 70(2023), 2221-2230.

[21] W. Liu, K. T. Chau, C. H. T. Lee, L. Cao and W. Han, *Wireless power and drive transfer for piping network*, IEEE Transactions on Industrial Electronics, ISSN 1557-9948, 69(2022), 2345-2356.

[22] W. Liu, K. T. Chau, H. Wang and T. Yang, *Long-range wireless power drive using magnetic extender*, IEEE Transactions on Transportation Electrification, ISSN 2332-7782, 9(2023), 1897-1909.

[23] M. Sato, G. Yamamoto, D. Gunji, T. Imura and H. Fujimoto, *Development of wireless in-wheel motor using magnetic resonance coupling*, IEEE Transactions on Power Electronics, ISSN 1941-0107, 31(2016), 5270-5278.

[24] A. Babaki, S. Vaez-Zadeh, A. Zakerian and A. Jafari Natanzi, *Analysis and control of wireless motor drives with a single inverter in primary side*, IEEE Transactions on Energy Conversion, ISSN 1558-0059, 36(2021), 930-939.

[25] Y. Chen, C. Gan, H. Shi, K. Ni, Z. Yang and R. Qu, *Auxiliary circuit free maximum power efficiency tracking scheme for wireless motor system with source-load coupling*, IEEE Transactions on Industrial Electronics, ISSN 1557-9948, 70(2023), 3414-3425.

[26] C. Li, Z. Wang and Y. Xu, *A wireless-power-transfer-based three-phase pmsm drive system with matrix converter*, IEEE Transactions on Industrial Electronics, ISSN 1557-9948, 70(2023), 2307-2317.

[27] H. Wang, K. T. Chau, C. H. T. Lee, L. Cao and W. H. Lam, *Design, analysis, and implementation of wireless shaded-pole induction motors*, IEEE Transactions on Industrial Electronics, ISSN 1557-9948, 68(2021), 6493-6503.

[28] H. Wang, K. T. Chau, C. H. T. Lee and C. Jiang, *Wireless shaded-pole induction motor with half-bridge inverter and dual-frequency resonant network*, IEEE Transactions on Power Electronics, ISSN 1941-0107, 36(2021), 13536-13545.

[29] W. Liu, K. T. Chau, C. H. T. Lee, C. Jiang, W. Han, and W. H. Lam, *Multi-frequency multi-power one-to-many wireless power transfer system*, IEEE Transactions on Magnetics, ISSN 1941-0069, 55(2019), 1-9.

[30] X. Tian, K. T. Chau, Z. Hua and W. Han, *Design and analysis of demand-customized selective wireless power transfer system*, IEEE Transactions on Industrial Electronics, ISSN 1557-9948, 69(2022), 13451-13461.

[31] X. Tian, K. T. Chau, W. Liu, H. Pang and C. H. T. Lee, *Maximum power tracking for magnetic field editing-based omnidirectional wireless power transfer*, IEEE Transactions on Power Electronics, ISSN 1941-0107, 37(2022), 12901-12912.

[32] C. Jiang, K. T. Chau, C. Liu, and W. Han, *Time-division multiplexing wireless power transfer for separately excited DC motor drives*, IEEE Transactions on Magnetics, ISSN 1941-0069, 53(2017), 1-5.

[33] X. Tian, K. T. Chau, H. Pang and W. Liu, *Power adaption design for multifrequency wireless power transfer system*, IEEE Transactions on Magnetics, ISSN 1941-0069,58(2022), 1-5.

[34] X. Hou, Z. Wang, Y. Su, Z. Liu, and Z. Deng, *A dual-frequency dual-load multi-relay magnetic coupling wireless power transfer system using shared power channel*, IEEE Transactions on Power Electronics, ISSN 0885-8993, 37(2022), 15717-15727.

[35] C. Jiang, K. T. Chau, W. Liu, C. Liu, W. Han and W. H. Lam, *An LCC-compensated multiple-frequency wireless motor system*, IEEE Transactions on Industrial Informatics, ISSN 1941-0050, 15(2019), 6023-6034.

[36] H. Wang, K. T. Chau, C. H. T. Lee, L. Cao and W. H. Lam, *Design, analysis, and implementation of wireless shaded-pole induction motors*, IEEE Transactions on Industrial Electronics, ISSN 1557-9948, 68(2021), 6493-6503.

[37] D. Ongayo and M. Hanif, *Comparison of circular and rectangular coil transformer parameters for wireless Power Transfer based on Finite Element Analysis*, 2015 IEEE 13th Brazilian Power Electronics Conference and 1st Southern Power Electronics Conference (COBEP/SPEC), Fortaleza, Brazil, 2015, 1-6.

[38] S. Li, W. Li, J. Deng, T. D. Nguyen and C. C. Mi, *A double-sided LCC compensation network and its tuning method for wireless power transfer*, IEEE Transactions on Vehicular Technology, ISSN 1939-9359, 64(2015), 2261-2273.

Presenter Biography

Songtao Li received the B.Eng. degree and M.Eng. degree both in instrument science and technology from Southeast University, Nanjing, China, in 2018 and 2021, respectively. He is currently working toward the Ph.D. degree in electrical and electronic engineering at The University of Hong Kong, Hong Kong, China. His research interests include power electronics, wireless power transfer, and motor drives.